Smart Materials and Devices
https://doi.org/10.70401/smd.2026.0029

Supplementary information

Regulating oxygen defects over CeO_2 via rare earth oxide doping for Pt-catalyzed oxidative dehydrogenation of propane with carbon dioxide

Chao Peng, Meng Yan, Zhong-Wen Liu

Table of Contents

1. TEM of PtSn/CeO2 catalyst

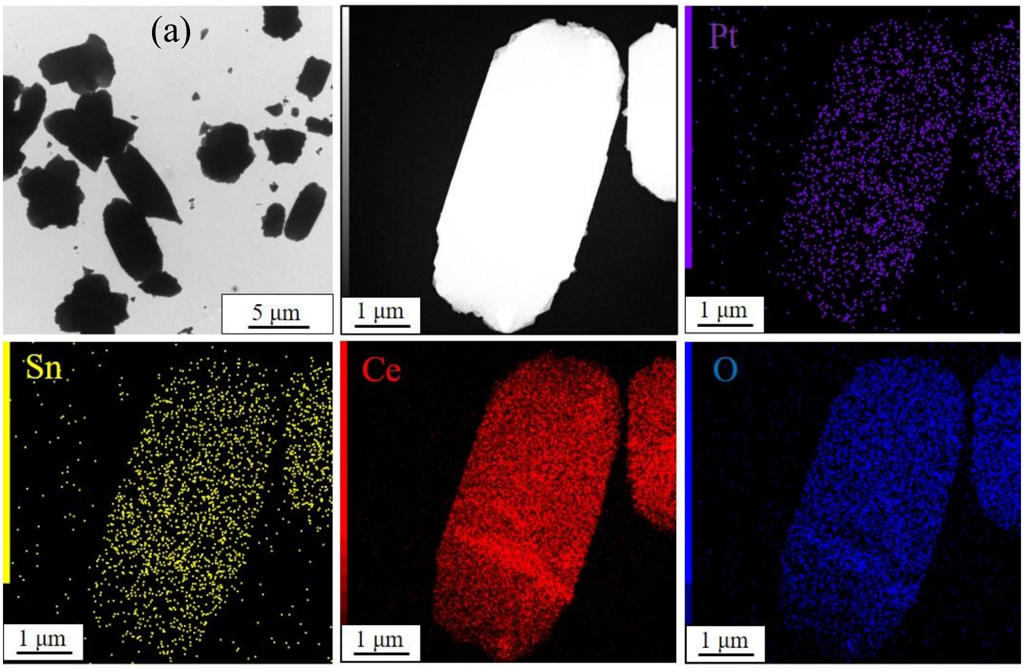

Figure S1. TEM images and STEM with EDS mapping of PtSn/CeO_2 catalyst. EDS: energy-dispersive X-ray spectroscopy.

2. Textural properties

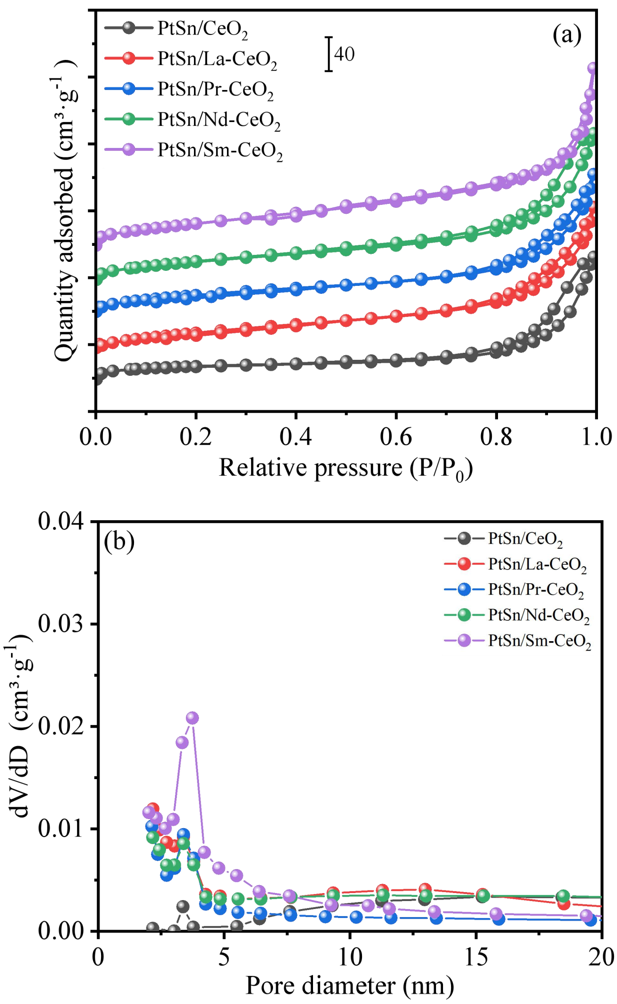

Figure S2. (a) N_2 adsorption–desorption isotherms and (b) pore-size distribution of undoped or RE-doped PtSn/CeO_2 catalysts.

3. XRD patterns of catalysts

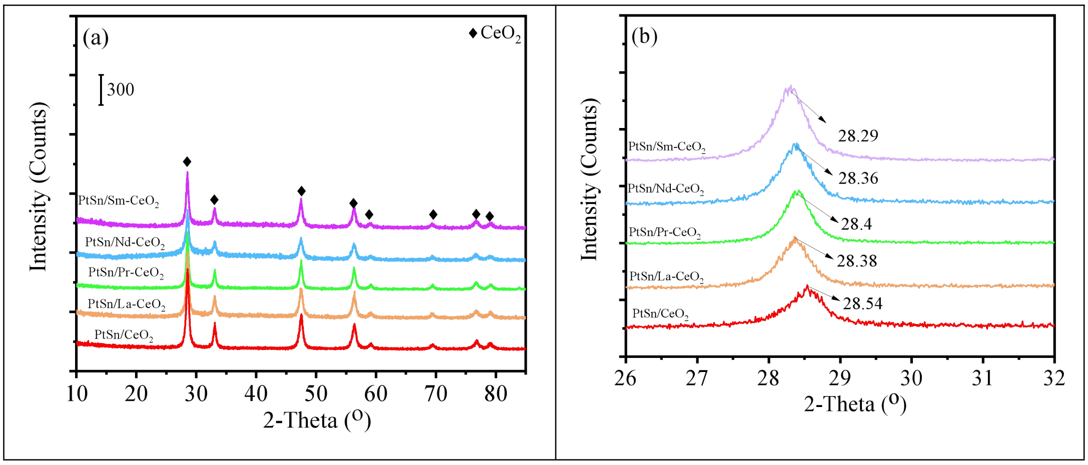

Figure S3 XRD patterns (a, b) over undoped or RE-doped PtSn/CeO_2 catalysts.

4. HRTEM of PtSn/CeO2 catalyst

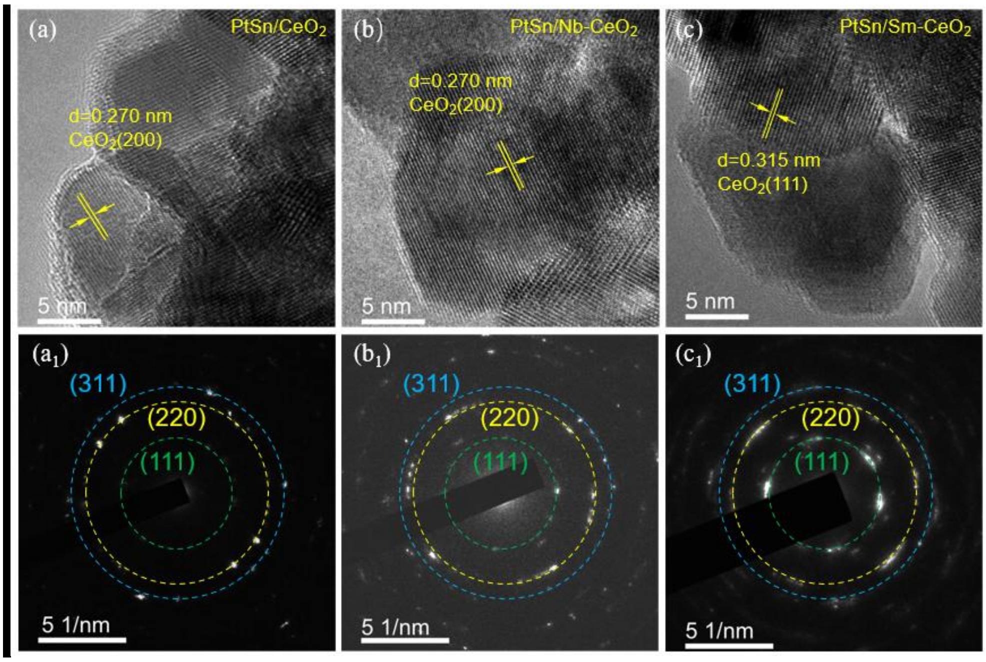

Figure S4. (a-c) HRTEM and (a_1-c_1) SAED images of PtSn/CeO_2, PtSn/Nb-CeO_2 and PtSn/Sm-CeO_2, respectively.

5. Raman spectra of catalysts

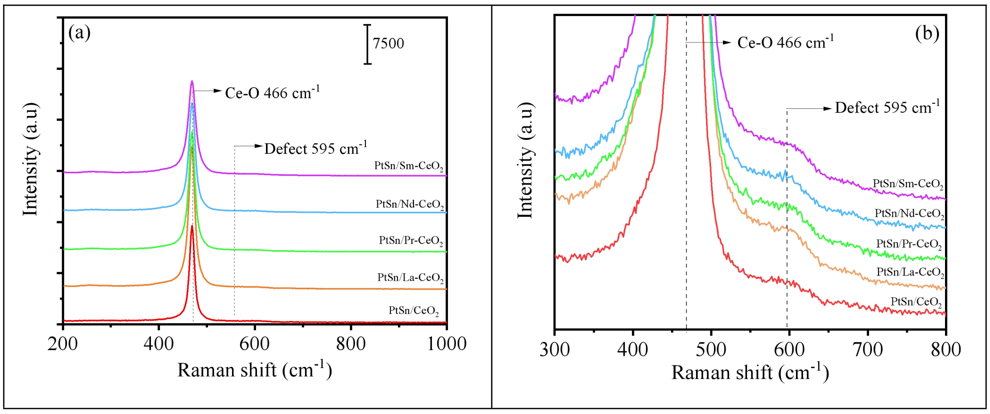

Figure S5. Raman spectra (a, b) over undoped or RE-doped PtSn/CeO_2 catalysts.

6. TOF of catalyst

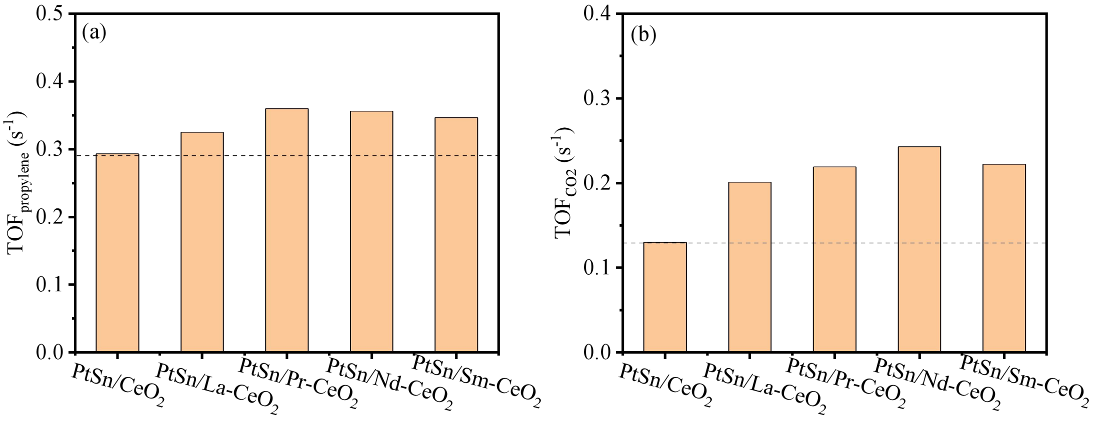

Figure S6. (a)$TOF_{propylene}$ and (b)TOF_{CO2} of undoped or RE-doped $PtSn/CeO_2$ catalysts.

7. The stability of PtSn/Nd-CeO2 catalyst

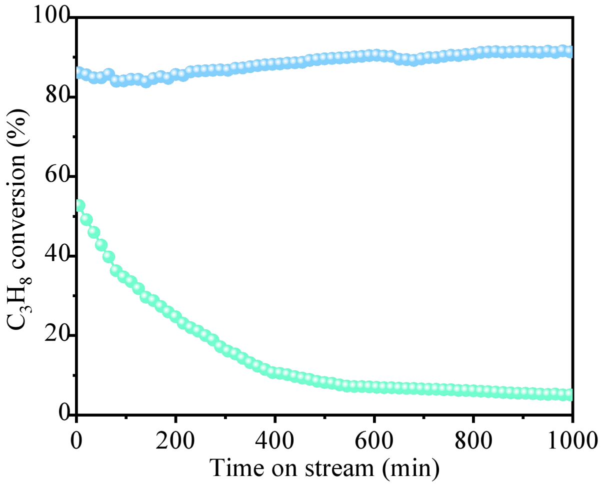

Figure S7. The stability of PtSn/Nd-CeO_2 catalyst for CO_2-ODP under the reaction conditions of T = 550 ℃, $m_{(cat.)}$ = 0.25 g, Ar/He/CO_2/C_3H_8 = 1:16:4:4, and total flow = 25 mL·min^{-1}.

8. Results of CO2-ODP over CeO2 and Nd-CeO2 supports

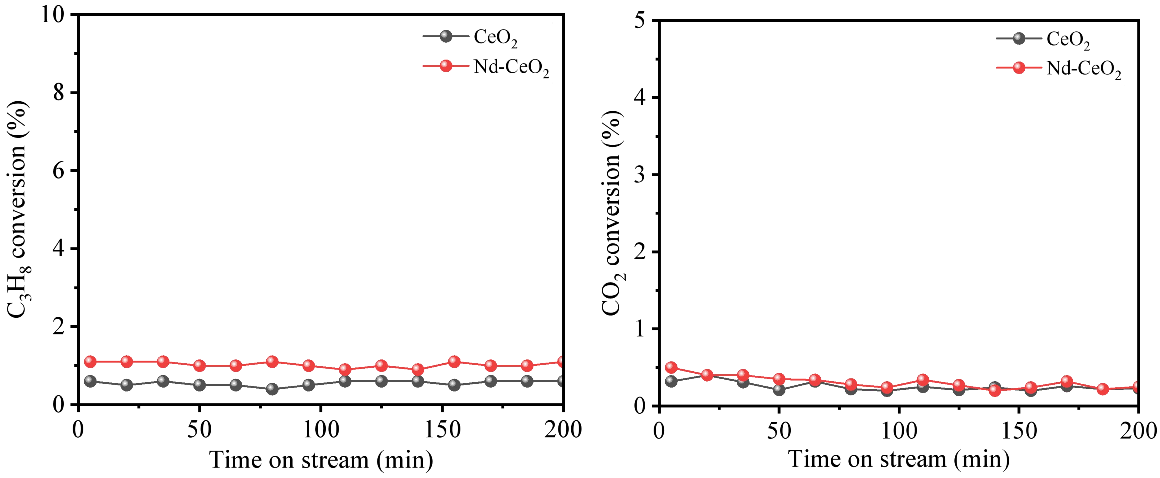

Figure S8. Time-on-stream C_3H_8 conversion and CO_2 conversion of CO_2-ODP over CeO_2 and Nd-CeO_2 supports under the reaction conditions of T = 550 ℃, $m_{(cat.)}$ = 0.1 g, Ar/He/CO_2/C_3H_8 = 1:16:4:4, total flow = 25 mL·min^{-1}.

9. The PDH and CO2-ODP performance of PtSn/Nd-CeO2 catalyst

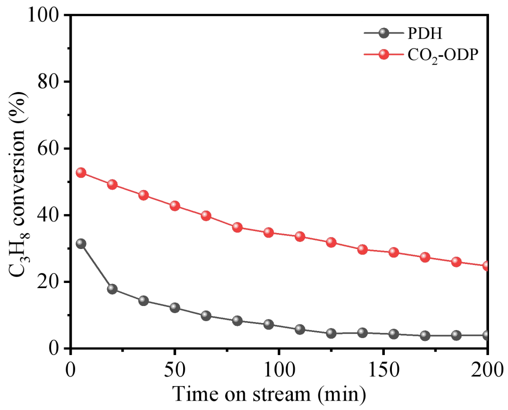

Figure S9. C_3H_8 conversion over PtSn/Nd-CeO_2 catalyst for PDH and CO_2-ODP reactions. (Reaction conditions for PDH: T = 550 ℃, $m_{(cat.)}$ = 0.25 g, Ar/He/C_3H_8 = 1/20/4, total flow = 25 mL·min^{-1}.; Reaction conditions for CO_2-ODP: T = 550 ℃, $m_{(cat.)}$ = 0.25 g, Ar/He/CO_2/C_3H_8 = 1/16/4/4, total flow = 25 mL·min^{-1}).

10. Transient MS responses of consecutive CO2 pulses

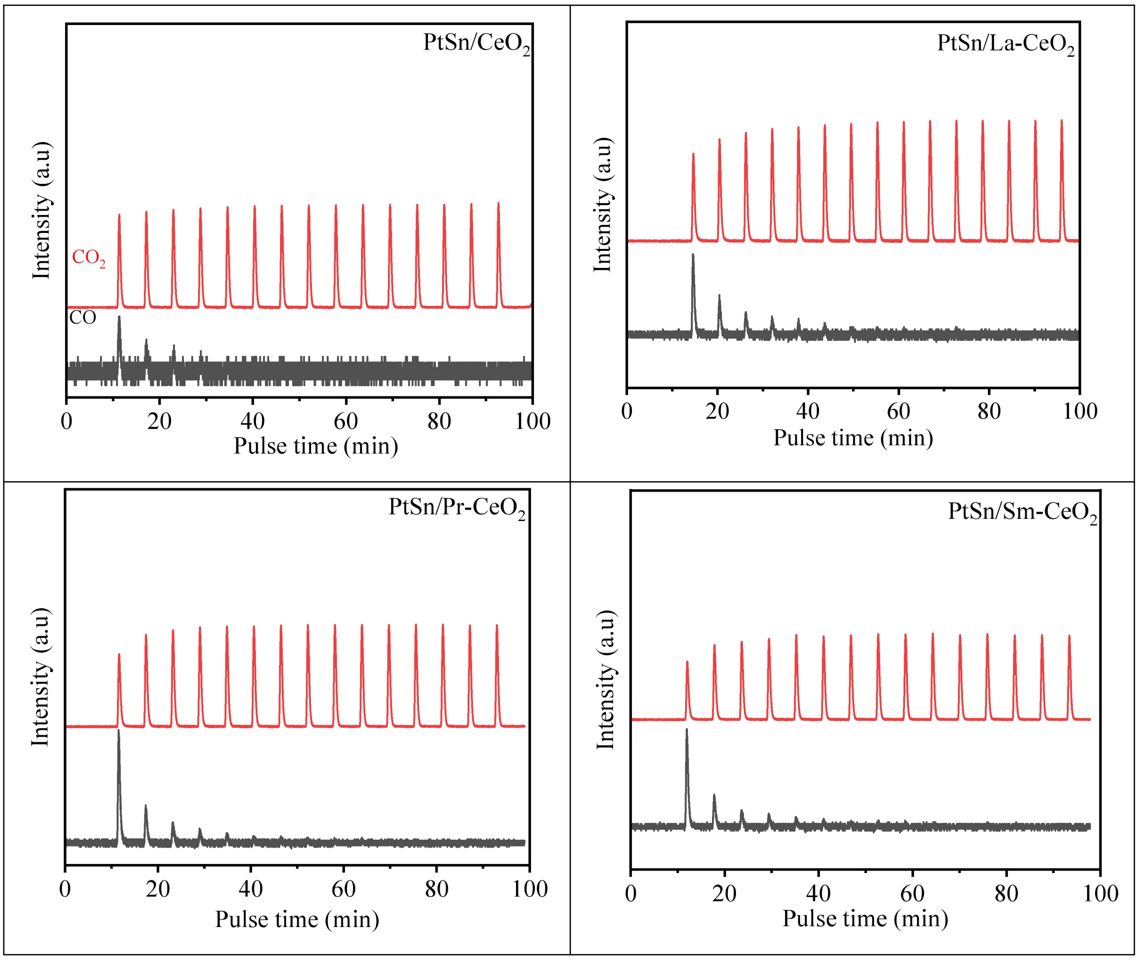

Figure S10. Transient MS responses of consecutive CO_2 pulses on the pre-reduced undoped or RE-doped $PtSn/CeO_2$ catalysts at 500 ℃ in 10% H_2 in Ar for 30 min.

11. Reaction mechanism of PtSn/Nd-CeO2 catalyst

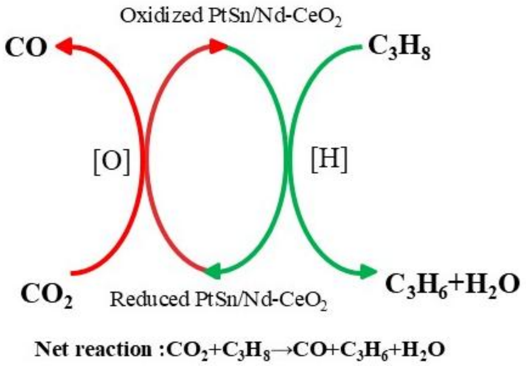

Figure S11. Schematic diagram of the oxidation-reduction cycles of the PtSn/Nd-CeO$_2$ catalyzed CO_2-ODP.

12. Carbon balance of catalysts

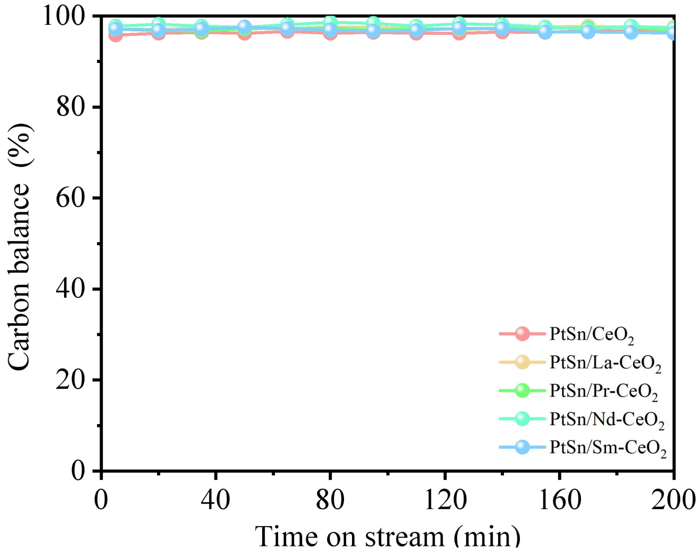

Figure S12. Time-on-stream carbon balance of CO_2-ODP over undoped or RE-doped PtSn/CeO_2 catalysts under the same reaction conditions to those in Figure 2.

13. Characterization results of spent catalysts

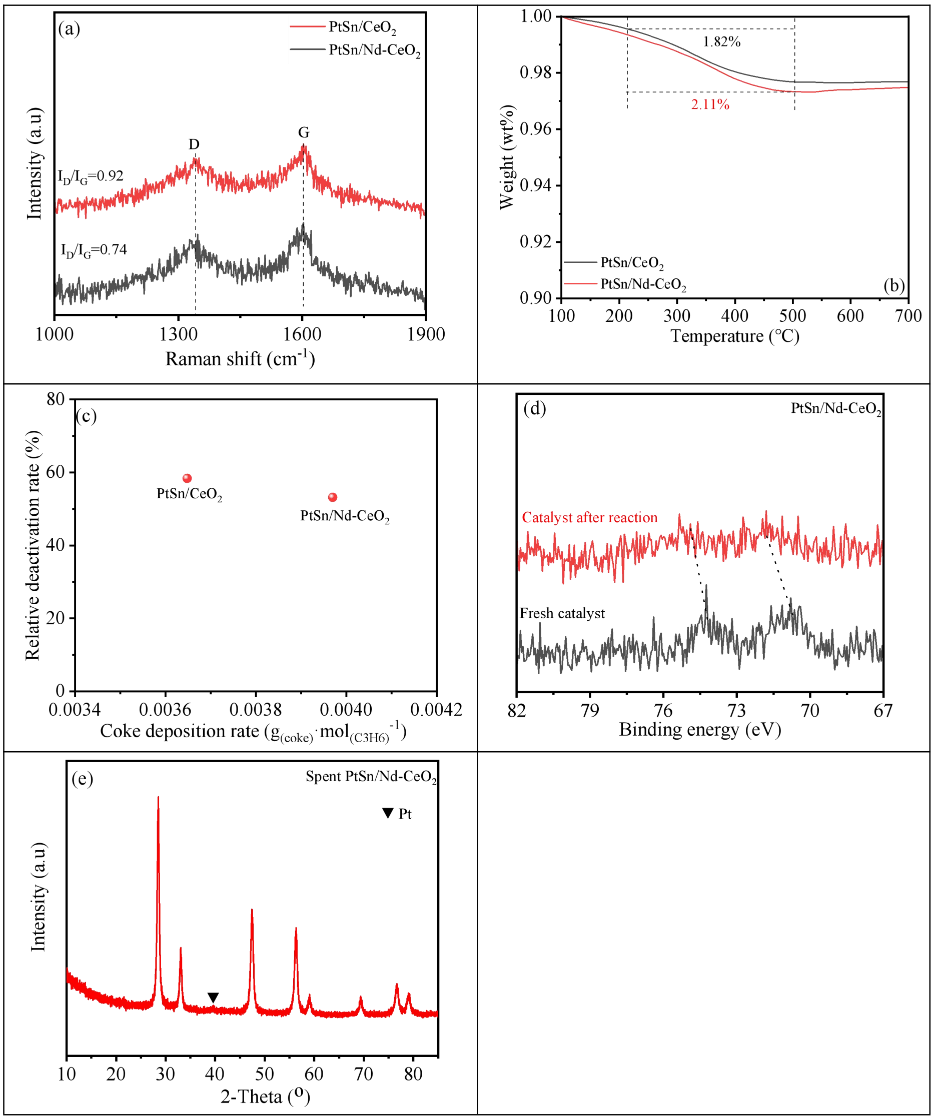

Figure S13. Raman spectra (a), TG profiles (b), correlation between relative deactivation rate and carbon deposition rate (c), Pt 4f XPS (d) and XRD patterns (e) of the spent $PtSn/CeO_2$ and $PtSn/Nd\text{-}CeO_2$ catalysts after CO_2-ODP for a TOS of 200 min.

14. The regeneration performance of PtSn/Nd-CeO2 catalyst

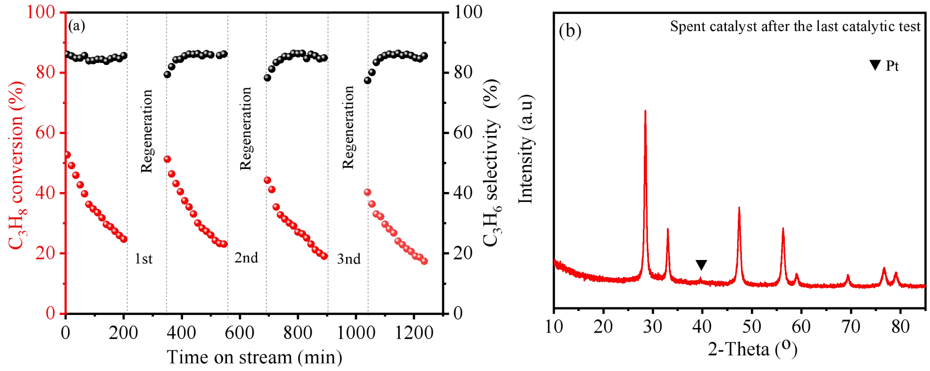

Figure S14. Reaction-regeneration performance of the PtSn/Nd-CeO_2 catalyst for CO_2-ODP (a) and the XRD pattern (b) of the spent catalyst after the last catalytic test. (Conditions for the regeneration and reduction: T = 500 ℃, air flow = 30 mL·min^{-1}, t = 30 min; T = 550 ℃, H_2 flow = 30 mL·min^{-1}, t = 60 min).

15. Synthesis conditions and measured CeO2 content of supports

Table S1. Textural and structural properties of $PtSn/CeO_2$ and $PtSn/RE\text{-}CeO_2$ catalysts.

Catalysts	CeO_2 particle size (nm)[a]	Specific surface area ($m^2 \cdot g^{-1}$)[b]	Pore volume ($cm^3 \cdot g^{-1}$)[c]	Average pore size (nm)
$PtSn/CeO_2$	17.8	49.9	0.105	10.0
$PtSn/La\text{-}CeO_2$	15.2	59.5	0.124	9.5
$PtSn/Pr\text{-}CeO_2$	14.5	56.5	0.118	9.6
$PtSn/Nd\text{-}CeO_2$	13.1	66.2	0.137	9.3
$PtSn/Sm\text{-}CeO_2$	13.9	64.4	0.133	9.1

a: Calculated from Scherrer's equation and the [111] diffraction of the cubic CeO_2 as given in the XRD patterns; b: Calculated by the BET method; c: Calculated from the cumulative volume of pores in diameter between 1.7 and 300 nm. BET: Brunauer-Emmett-Teller.

16. Calculated Ce 3d and O 1s XPS results

Table S2. The relative percent of surface Pt, Sn and Ce with different chemical states derived from XPS analyses.

Catalyst	Ce species (%)		O species (%)
	$Ce^{3+}/(Ce^{3+}+Ce^{4+})$	Ce^{3+}/Ce^{4+}	$O_\beta/(O_\alpha+O_\beta+O_\gamma)$
PtSn/CeO_2	13.4	15.5	24.1
PtSn/La-CeO_2	19.7	24.5	33.2
PtSn/Pr-CeO_2	21.3	27.1	36.7
PtSn/Nd-CeO_2	26.7	36.4	44.6
PtSn/Sm-CeO_2	23.4	30.5	39.9

17. Synthesis conditions and measured CeO2 content of supports

Table S3. Textural and structural properties of PtSn/CeO_2 and PtSn/RE-CeO_2 catalysts.

Catalysts	Pt dispersion (%)	Pt loading (wt.%)[a]
PtSn/CeO_2	22.1	0.99
PtSn/La-CeO_2	24.6	0.98
PtSn/Pr-CeO_2	25.7	0.97
PtSn/Nd-CeO_2	30.4	0.98
PtSn/Sm-CeO_2	28.5	0.97

a: Determined by ICP-MS

18. Calculated Pt 4f and Sn 3d XPS results

Table S4. The relative percent of surface Pt and Sn with different chemical states derived from XPS analyses.

Catalyst	Pt species (%)		Sn species (%)					
	$Pt^0/(Pt^0+Pt^{2+})$	Pt^0/Pt^{2+}	Sn^0 (eV)	Sn^0 Peak area	$Sn^{2+/4+}$ (eV)	$Sn^{2+/4+}$ Peak area	$Sn^0/(Sn^0+Sn^{2+/4+})$	$Sn^0/Sn^{2+/4+}$
PtSn/CeO_2	30.5	43.9	484.7	80.8	486.4	636.2	11.3	12.7
PtSn/La-CeO_2	34.8	53.4	484.6	90.1	486.3	566.7	13.7	15.9
PtSn/Pr-CeO_2	36.7	58.0	484.8	84.9	486.2	485.1	14.9	17.5
PtSn/Nd-CeO_2	38.9	63.7	484.6	72.1	486.2	346.6	17.2	20.8
PtSn/Sm-CeO_2	37.8	60.8	484.6	76.8	486.3	400.1	16.1	19.2

19. Reaction conditions and main results of CO2-ODP over different catalysts

Table S5. Reaction conditions and main results of CO_2-ODP over different CeO_2-containing catalysts.

Catalyst	T (℃)	Reaction conditions				Initial C_3H_6 yield (%)	Initial STY[a]	CO_2 conversion (%)	Ref..
		Gas feed ratio	Total flow (ml·min^{-1})	Catalyst loadings (g)	TOS (min)				
Fe_3Ni/CeO_2	550	C_3H_8: CO_2: He=1:1:2	40.0	0.1	600	1.60	0.18	12.0-5.7	[1]
$FeCeO_2$	550	C_3H_8: CO_2: He=5:5:90	30.0	0.2	1200	8.40	0.07	N/A	[2]
FeNi/Ceria-Vo-R	550	C_3H_8: CO_2: He=2.4:4.8:10	17.2	1.0	180	9.66	0.03	N/A	[3]
5% Cr/$Ce_{0.2}Zr_{0.8}O_2$	600	C_3H_8: CO_2: He=0.5:1:18.5	20.0	0.2	360	49.7	0.14	31.2	[4]
5 C rO_y/e$_{0.5}$Zr$_{0.5}O_2$/SiO_2-wet	675	C_3H_8: CO_2=1:2	30.0	0.5	N/A	29.0		N/A	[5]
5Pd/CeZrAlO_x	500	C_3H_8: CO_2: He=37:37:26	15.0	0.2	8400	13.0	0.41	N/A	[6]
3%Pt-Co-In/CeO_2	550	C_3H_8: CO_2: He=1:1:2	20.0	0.1	1200	47.0	2.64	40-50	[7]
HEI/CeO_2	600	C_3H_8: CO_2: He=1:1:2	20.0	0.1	3000	28.2	1.58	53-24	[8]
PtSn/Ce-DMSN-0.5	550	C_3H_8: CO_2: He:Ar=8:8:8:1	25.0	0.1	2000	38.3	3.45	21.7-12.2	[9]
1Pt5Sn/CeO_2	500	C_3H_8: CO_2: N_2: Ar=4:4:16:1	50.0	0.50	80	15.9	0.03	N/A	[10]
PtSn/SH-CeO_2	550	C_3H_8: CO_2: He:Ar=4:4:16:1	25.0	0.25	200	39.4	0.71	42.3-22.3	[11]
PtSn/Nd-CeO_2	550	C_3H_8: CO_2: He:Ar=4:4:16:1	25.0	0.25	200	45.3	0.82	31.6-15.7	This work

a: STY is for the space-time yield of propene with the unit of kg$_{(C3H6)}$·kg$^{-1}_{(cat)}$·h^{-1}.

20. References

1.Gomez E, Kattel S, Yan B, Yao S, Liu P, Chen JG. Combining CO_2 reduction with propane oxidative dehydrogenation over bimetallic catalysts. Nat Commun. 2018;9:1398. [DOI:10.1038/s41467-018-03793-w]

2.Wang H, Tsilomelekis G. Catalytic performance and stability of Fe-doped CeO_2 in propane oxidative dehydrogenation using carbon dioxide as an oxidant. Catal Sci Technol. 2020;10(13):4362-4372. [DOI:10.1039/d0cy00586j]

3.Wang Y, Zhang Z, Lei L, Liu W, Du S, Zhu X, et al. Defect-dependent selective C−H/C−C bond cleavage of propane in the presence of CO_2 over FeNi/ceria catalysts. ACS Sustain Chem Eng. 2021;9(51):17301-17309. [DOI:10.1021/acssuschemeng.1c06095]

4.Dou J, Funderburg J, Yang K, Liu J, Chacko D, Zhang K, et al. $Ce_xZr_{1-x}O_2$-supported CrO_x catalysts for CO_2-assisted oxidative dehydrogenation of Propane—Probing the active sites and strategies for enhanced stability. ACS Catal. 2023;13(1):213-223. [DOI:10.1021/acscatal.2c05286]

5.Mashkin MY, Tedeeva MA, Fedorova AA, Fatula ER, Egorov AV, Dvoryak SV, et al. Synthesis of $Ce_xZr_{1-x}O_2/SiO_2$ supports for chromium oxide catalysts of oxidative dehydrogenation of propane with carbon dioxide. J Chem Tech Biotech. 2023;98(5):1247-1259. [DOI:10.1002/jctb.7339]

6.Nowicka E, Reece C, Althahban SM, Mohammed KMH, Kondrat SA, Morgan DJ, et al. Elucidating the role of CO_2 in the soft oxidative dehydrogenation of propane over ceria-based catalysts. ACS Catal. 2018;8(4):3454-3468. [DOI:10.1021/acscatal.7b03805]

7.Xing F, Nakaya Y, Yasumura S, Shimizu KI, Furukawa S. Ternary platinum−cobalt−indium nanoalloy on ceria as a highly efficient catalyst for the oxidative dehydrogenation of propane using CO_2. Nat Catal. 2022;5(1):55-65. [DOI:10.1038/s41929-021-00730-x]

8. Xing F, Ma J, Shimizu KI, Furukawa S. High-entropy intermetallics on ceria as efficient catalysts for the oxidative dehydrogenation of propane using CO_2. Nat Commun. 2022;13(1):5065. [DOI:10.1038/s41467-022-32842-8]

9.Peng C, Yang GQ, Ge HQ, Liu YF, Liu ZW. PtSn supported on CeO_2 modified dendritic mesoporous SiO_2 as an efficient catalyst for oxidative dehydrogenation of propane with CO_2. Appl Catal B Environ Energy. 2026;385:126243. [DOI:10.1016/j.apcatb.2025.126243]

10.Yang GQ, Ren X, Kondratenko VA, Zhang HB, Kondratenko EV, Liu ZW. Promotional nature of Sn on Pt/CeO_2 for the oxidative dehydrogenation of propane with carbon dioxide. Nano Res. 2023;16(5):6237-6250. [DOI:10.1007/s12274-022-5316-0]

11.Peng C, Yang G, Ge H, Liu Z. Morphology engineered PtSn/CeO_2 catalysts for oxidative dehydrogenation of propane with carbon dioxide. J Rare Earths. 2025. [DOI:10.1016/j.jre.2025.07.022]